

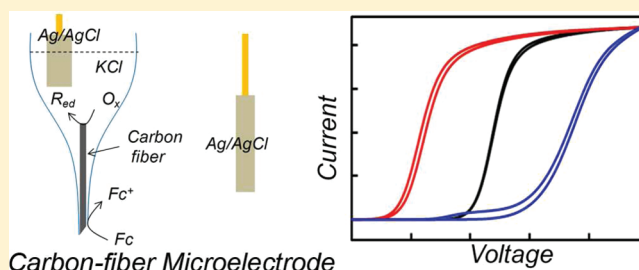
Coupled Electrochemical Reactions at Bipolar Microelectrodes and Nanoelectrodes

Joshua P. Guerrette, Stephen M. Oja,[†] and Bo Zhang*

Department of Chemistry, University of Washington, Seattle, Washington 98195-1700, United States

S Supporting Information

ABSTRACT: Here we report the voltammetric study of coupled electrochemical reactions on microelectrodes and nanoelectrodes in a closed bipolar cell. We use steady-state cyclic voltammetry to discuss the overall voltammetric response of closed bipolar electrodes (BPEs) and understand its dependence on the concentration of redox species and electrode size. Much of the previous work in bipolar electroanalytical chemistry has focused on the use of an “open” cell with the BPE located in an open microchannel. A closed BPE, on the other hand, has two poles placed in separate compartments and has remained relatively unexplored in this field. In this work, we demonstrated that carbon-fiber microelectrodes when backfilled with an electrolyte to establish conductivity are closed BPEs. The coupling between the oxidation reaction, e.g., dopamine oxidation, on the carbon disk/cylinder and the reduction of oxygen on the interior fiber is likely to be responsible for the conductivity. We also demonstrated the ability to quantitatively measure voltammetric properties of both the cathodic and anodic poles in a closed bipolar cell from a single cyclic voltammetry (CV) scan. It was found that “secondary” reactions such as oxygen reduction play an important role in this process. We also described the fabrication and use of Pt bipolar nanoelectrodes which may serve as a useful platform for future advances in nanoscale bipolar electrochemistry.



Carbon-fiber Microelectrode

Electroanalytical chemists have recently become interested in the unique properties of bipolar electrodes (BPEs) and their application toward novel sensing and separation systems.^{1,2} Several interesting studies have been published lately, predominantly by the Crooks group, discussing new detection schemes^{3–6} and new applications of BPEs in sensing⁷ and separation.⁸ Previous work, however, has primarily focused on the use of open bipolar systems in which a BPE or an array is placed inside a microfluidic channel. Scheme 1a illustrates a cartoon of a typical open bipolar cell containing a pair of driving electrodes to apply a voltage along the length of the channel which polarizes the electrode. A significant portion of the total current between the driving electrodes is carried by an ionic current within the microchannel. As such, the electrochemical reaction rate on the BPE in general cannot be monitored by the current in the external circuit. The voltage needed to achieve the desired faradic response is inversely proportional to the length of the BPE¹ and can be quite large for certain applications.

A closed bipolar electrode⁹ eliminates the microfluidic path, thus completely separating the two poles in two different compartments. Scheme 1b displays the basic design of a closed bipolar cell, which also uses two driving electrodes to supply a voltage across the two separated solutions. This voltage is dropped almost entirely at the solution interface adjacent to the two ends of the BPE when two ideal nonpolarizable electrodes, e.g., Ag/AgCl electrodes, are used. A relatively small voltage (<1 V) is normally sufficient to drive both redox reactions on the BPE. In this case the entire electrical current must pass

through the BPE and can therefore be used to report the rates of the faradic processes on the BPE. In this study we limit our discussion to closed BPEs. This system is analogous to two series-coupled electrochemical cells, as recently described by Plana et al.¹⁰ Such cells have been used to study electron transfer at liquid/liquid interfaces^{10–12} and electroless deposition.¹³

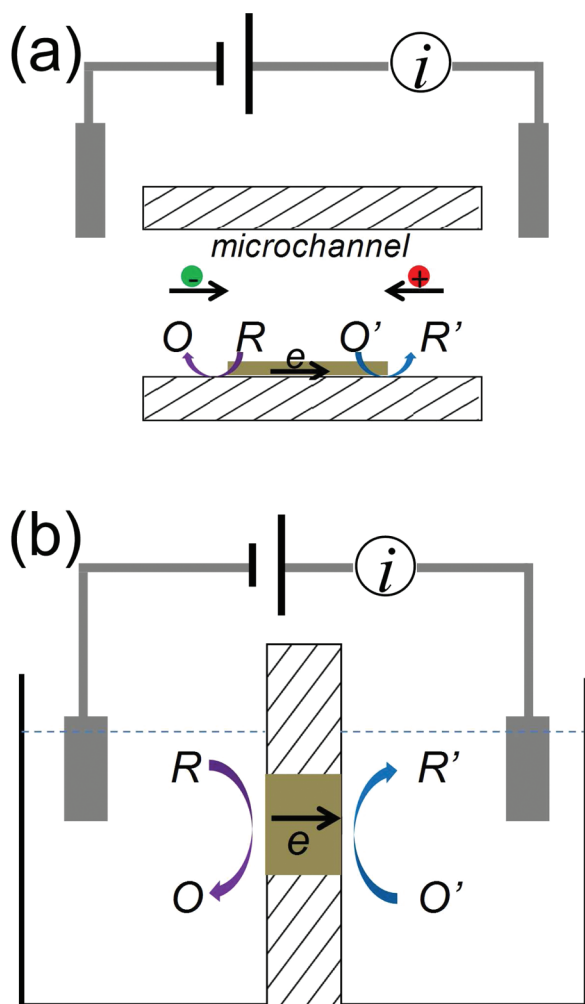
It is important to note that one of the most common examples of a closed BPE used in electroanalytical chemistry, although not previously described as such, could be the carbon-fiber microelectrode (CFE). CFEs are routinely used for both single-cell studies¹⁴ and in vivo experiments.¹⁵ These electrodes are usually prepared by sealing a small carbon fiber in a pulled glass capillary pipet. The fiber is then beveled or cut to obtain a disk or cylinder electrode. Although other means exist,¹⁶ electrical conductivity on the interior pipet is often established by backfilling the capillary with an aqueous solution of KCl^{17,18} or potassium acetate^{19,20} and inserting a Ag or steel wire.²¹ This procedure is advantageous because it facilitates rapid change of CFEs between cell experiments. It is assumed that the rate of electron transfer on the interior fiber is capable of occurring in sufficient excess to allow for quantitative measurements limited solely by the oxidation reaction at the carbon electrode. We believe that this assumption may not always be true and that a

Received: November 2, 2011

Accepted: January 9, 2012

Published: January 9, 2012

Scheme 1. Comparison of an Open Bipolar Cell (a) and a Closed Bipolar Cell (b)



deeper investigation into the redox coupling at closed BPEs is necessary to improve the reliability of such measurements.

In this report we start by investigating the voltammetric response of CFEs. We then focus on a simplified setup in which two electrochemical cells are coupled in series. This setup allows us to use well-characterized Au and Pt microelectrodes and nanoelectrodes connected in series to obtain a more detailed understanding of the voltammetric behavior of closed bipolar microelectrodes. We then return our discussion to CFEs and the voltammetric detection of dopamine (DA). Through this investigation we begin to understand the role of secondary reactions (i.e., the oxidation of water and reduction of oxygen) in the response of BPEs in aqueous solutions. We demonstrate the ability to obtain quantitative information (such as electrode size or redox concentration) about both poles of a closed bipolar cell in a single voltammetric scan. Finally we briefly discuss the use of bipolar nanoelectrodes.

EXPERIMENTAL SECTION

Chemicals. Potassium ferricyanide ($K_3Fe(CN)_6$, Sigma-Aldrich), potassium ferrocyanide ($K_4Fe(CN)_6$, Fluka), ferrocene (Fc, Fluka Analytical), ferrocenemethanol (FcMeOH, Aldrich), dopamine hydrochloride (DA, Sigma-Aldrich), hexaamineruthenium(III) chloride ($Ru(NH_3)_6Cl_3$, Aldrich), tetra-*n*-butylammonium hexafluorophosphate (TBAPF₆,

Aldrich), KCl (J.T. Baker), sodium sulfate (Na_2SO_4 , Fisher Chemicals), perchloric acid ($HClO_4$, Aldrich), and reagent grade MeCN (Aldrich) were all used without further purification. A Barnstead Nanopure water purification system was used to provide $>18\text{ M}\Omega\cdot\text{cm}$ deionized water for all aqueous solutions.

Fabrication of CFEs and Pt Bipolar Nanoelectrodes. CFEs were fabricated following our previously reported procedures.²² Briefly, an isolated carbon fiber ($5\ \mu\text{m}$ diameter) was aspirated into a borosilicate glass capillary (1.2 mm o.d., 0.69 mm i.d., Sutter). Capillaries were subsequently pulled with a P-97micropipet puller (Sutter) and sealed with epoxy (Epoxy Technology) and beveled to 45° or further sealed in epoxy and polished at 90° as noted. Pt bipolar nanoelectrodes were prepared by sealing a short piece of quartz-coated Pt nanowire²³ in a glass micropipet (see the Supporting Information for additional details).

Cyclic Voltammetry. A four-electrode, two-cell setup equipped with two working electrodes and two Ag/AgCl electrodes (Bioanalytical Sciences Inc.) was used in all series-coupled bipolar electrochemical experiments (see Figure 2a). Two AgCl-coated Ag wire quasi-reference electrodes were used for pipet-based bipolar nanoelectrodes. Cyclic voltammetry (CV) was carried out using a Chem-Clamp potentiostat (Dagan) connected to an EG&G 175 programmer. CV response was recorded using a PCI-6251(National Instruments) card on a Dell PC using in-house LabView 8.5 software (National Instruments). A scan rate of 50 mV/s was used for all CV experiments unless noted otherwise.

Scanning Electron Microscopy. Scanning electron microscopy (SEM) images presented in the Supporting Information file were obtained using a field-emission microscope (FEI Sirion). Samples were sputter-coated with a thin layer (2–3 nm) of Au/Pd prior to imaging.

RESULTS AND DISCUSSION

In the following sections several redox species are discussed in different series-coupled combinations. Supporting Information Table S11 provides a summary of experimental half-wave potentials and diffusion coefficients used for calculations and comparisons involving relative limiting factor.

CFEs as Closed Bipolar Electrodes. A literature search regarding CFEs will not yield any mention of bipolar electrochemistry nor will one find a detailed discussion of the mechanism by which CFEs achieve conductivity when backfilled with an electrolyte solution. Figure 1a is a schematic diagram of a CFE, in which Fc is oxidized at the carbon disk and electrons flow through the fiber into the inner capillary. *The oxidation of Fc (or DA) must be balanced through the reduction of another redox species at the interior fiber due to electroneutrality, which makes CFE a good example of bipolar electrode.* We believe oxygen reduction reaction (ORR) may be responsible for the establishment of conductivity and therefore sought to investigate this further.

We have found that the CV response of a KCl-filled CFE can often be distorted with significant variability in the half-wave potential, $E_{1/2}$, for a given redox molecule. This behavior may be due to electrochemical limitations on the interior fiber. Figure 1b shows a typical CV of a $5\ \mu\text{m}$ diameter CFE beveled at a 45° angle in MeCN containing 5 mM Fc and 0.1 M TBAPF₆. A 3 M KCl solution is used to establish electrical conductivity (black). A sigmoidal CV response is obtained with a limiting current of 22 nA and an $E_{1/2}$ of 0.48 V versus

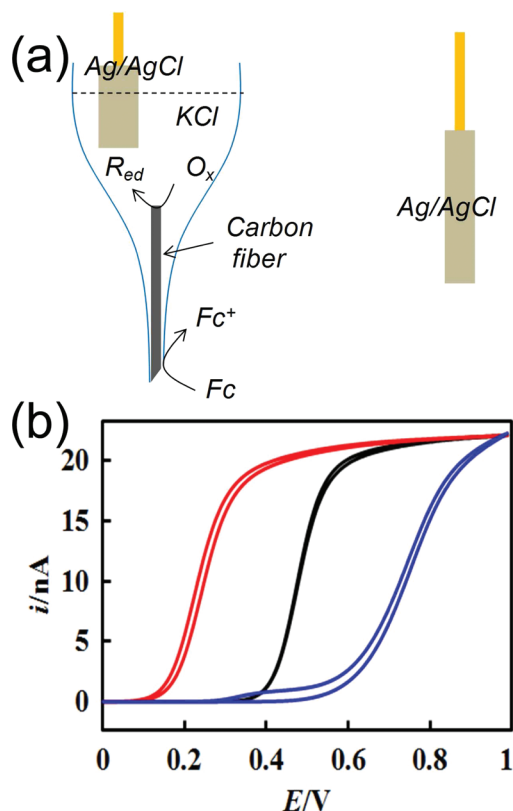


Figure 1. (a) Schematic diagram of a CFE being used to study the oxidation of Fc. A KCl solution is used to establish the conductivity in the capillary. (b) Voltammetric response of a 5 μm diameter CFE in 5 mM Fc, 0.1 M TBAPF₆ in MeCN. Electrical conductivity inside of the CFE was made with 3 M KCl (black) and 5 mM Fe(CN)₆³⁻ in 0.1 M KCl (red). The blue CV was obtained from a second CFE with 3 M KCl on the inside showing a typical distortion.

Ag/AgCl. The blue CV is the response of another similarly prepared CFE in the same Fc solution. This CV shows a typical distortion seen with CFEs of this design: the current due to Fc oxidation increases much slower producing an $E_{1/2}$ almost 300 mV higher than the other electrode (black). An electrode with such response is often discarded in single-cell studies due to its slow behavior; however, it is unclear what causes this slower response. In order to demonstrate the importance of understanding the faradaic process on the internal carbon, for the electrode whose CV is shown in black, the internal solution was replaced by 5 mM Fe(CN)₆³⁻ with 0.1 M KCl (Figure 1b, red). This CV displays a similar sigmoidal response as the black curve; however, the $E_{1/2}$ has shifted nearly 250 mV negatively. We believe that the oxidation of Fc is now coupled to the reduction of ferricyanide which requires less external driving force than before.

We suggest that the outside carbon disk and the internal fiber are the anodic pole and the cathodic pole of a closed BPE, respectively. We also suggest that the reduction of oxygen is responsible for the reduction process at the cathodic pole for KCl-filled CFEs (vide infra). In general, the overall voltammetric response of a CFE is determined by the size and shape of exterior carbon electrode and only weakly dependent on the interior fiber or the composition of the inner solution because the interior fiber is typically much greater than the outside. However, if the maximum faradaic current on the interior fiber becomes limited due to a smaller fiber length or

the depletion of oxygen, the voltammetric response of the CFE may be significantly altered. In the next section, we show that oxygen reduction is not sufficient to keep up with the external carbon in size. The addition of a fast redox mediator, e.g., Fe(CN)₆³⁻, seems to be beneficial because it is easier to maintain a higher concentration and can decrease the overall applied voltage.

Use of Closed Bipolar Cells Involving Two Microelectrodes. There are two main difficulties in using a standard pipet-based CFE in this study. The first is the inherent challenge in controlling the size of the interior fiber, and the second is the inability to completely replace the internal solution within the confines of the capillary. A simplified experimental setup was chosen which connects two separate two-electrode cells in series. A diagram of this setup is presented in Figure 2a. The two electrodes labeled WE1 and

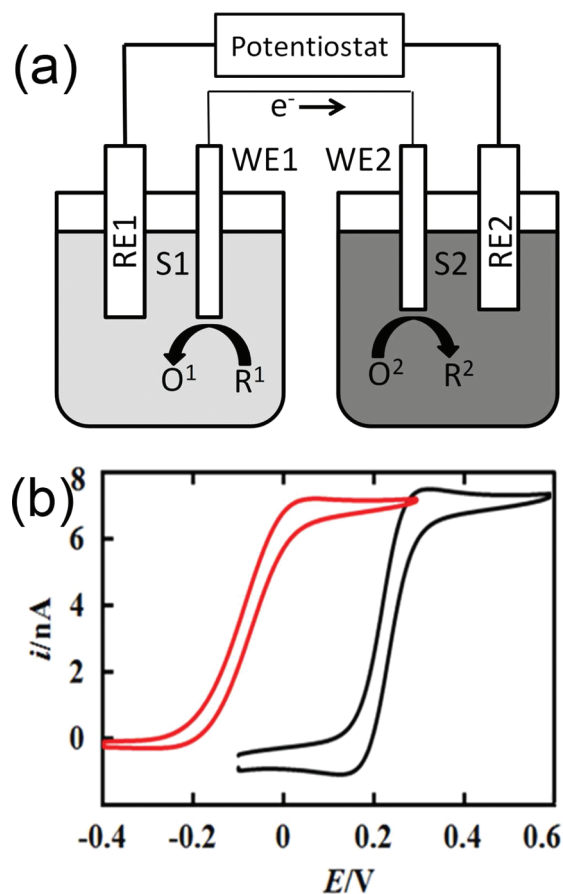


Figure 2. (a) Schematic showing the simplified cell configuration of a closed bipolar microelectrode. (b) Cyclic voltammetric response of a 25 μm diameter Au electrode in 2 mM FcMeOH in 0.1 M Na₂SO₄. The black CV shows the oxidation of FcMeOH on the 25 μm diameter Au electrode with a conventional one-compartment cell vs a Ag/AgCl reference electrode. The red CV was obtained on the same electrode using a closed bipolar cell as shown in panel a. A 12.5 μm diameter Au electrode in 5 mM Fe(CN)₆³⁻, 3 M KCl was used for the second compartment.

WE2 are used as the two ends of a closed bipolar cell. With this setup, the solution composition and the relative size of the poles can now be freely controlled.

Figure 2b is a comparison between the CV response of a 25 μm diameter Au disk electrode (black) in 2 mM FcMeOH

and 0.1 M Na₂SO₄ in a conventional one-compartment cell and that of the same electrode in a bipolar cell (red). In the bipolar setup, this electrode was connected to a 12.5 μm diameter Au electrode placed in 5 mM Fe(CN)₆³⁻ and 3 M KCl, as shown in Figure 2a. Although the electrode in the FcMeOH solution has a diameter twice as large, the lower concentration of FcMeOH and smaller diffusion coefficient ($D \approx 0.67 \times 10^{-5}$ cm²/s)²⁴ than ferricyanide ($D \approx 0.76 \times 10^{-5}$ cm²/s)²⁵ result in a lower mass transfer rate to the larger electrode. Both CVs are therefore limited by the oxidation of FcMeOH on the 25 μm diameter Au electrode. The $E_{1/2}$ of the bipolar setup is, however, 330 mV more negative than that in the conventional experiment. Similar to the analysis used by Plana et al. to study macroscopic electrodes, the $E_{1/2}$ of the bipolar microelectrode is directly related to the redox reactions on the two poles of the BPE and can be estimated from the difference in the formal redox potentials, ΔE° :

$$E_{1/2} \approx \Delta E^\circ = E^\circ_c - E^\circ_a \quad (1)$$

where E°_c and E°_a are the formal redox potentials for the cathode and anode, respectively. Because the formal potentials are generally close to the half-wave potentials for reversible processes,²⁶ one can also use $\Delta E_{1/2}$ to estimate the $E_{1/2}$ of a closed bipolar microelectrode. In this case, the oxidation of FcMeOH in 0.1 M Na₂SO₄ has an $E_{1/2}$ of 0.22 V versus Ag/AgCl, whereas the reduction of ferricyanide occurs at 0.32 V versus Ag/AgCl (see Supporting Information Figure S11), which yields an expected $E_{1/2}$ of -0.10 V for the BPE as was observed in Figure 2b. As we will demonstrate later, additional factors must be considered to estimate the $E_{1/2}$ when the maximum limiting currents on the two poles differ greatly.

The series-coupled bipolar setup was used to investigate the behavior of CFEs in the oxidation of DA and the role of ORR. To accomplish this, direct electrical connection was made to the interior fiber of a 5 μm diameter CFE using Ag paste and a tungsten wire. This electrode was connected in series either to an identically prepared disk electrode to create a CF BPE with two equal area poles or to a 5 μm diameter CF cylinder of variable length to create an electrode analogous to that shown in Figure 1a. Figure 3 shows the CV response of an electrode of

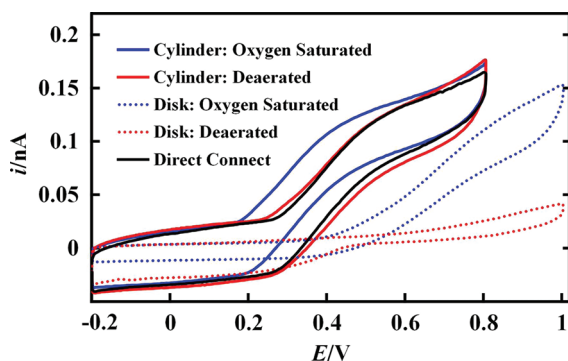


Figure 3. Cyclic voltammograms showing the oxidation of DA at a 5 μm diameter CF disk in a series-coupled bipolar configuration similar to that of Figure 2a. The cathodic pole was a 5 μm diameter CF cylinder of 7 mm in length (solid lines, red and blue) or another 5 μm diameter CF disk (dotted lines, blue and red) in a solution containing 3 M KCl. The black trace shows the response when the CF is directly connected to the working electrode lead using silver paste and a tungsten wire.

this design in an isotonic saline solution containing 100 μM DA and 1 mM HClO₄. The CVs obtained with the disk electrode

connected in series to a 7 mm length cylinder in 3 M KCl, both oxygen-saturated and deaerated with argon (blue and red solid lines, respectively), show a very similar response to that of a setup using the directly connected electrode (black). Although the oxygen-saturated solution requires a slightly lower driving potential than the others, the deaerated 3 M KCl solution still provides sufficient current to reach the same limiting current. When this electrode is connected in series to another 5 μm diameter disk, the response (dotted lines) is significantly different. The combined detrimental effects of the smaller electroactive area as well as the lower oxygen concentration of the deaerated solution lead to insufficient reduction current on the cathodic pole producing a response that is now unrepresentative of the DA oxidation. The smaller cathodic pole is only capable of achieving a response limited by the DA oxidation at the anodic pole if the solution is oxygenated and a higher potential is applied (blue dotted line). With the larger cylinder electrode, the reduction of low concentrations of residual oxygen in solution and the presence of reducible contaminants provide a sufficient cathodic current. Supporting Information Figure SI2 shows the CV response of the oxidation of DA coupled to the reduction of 5 mM ferricyanide using two 5 μm disks in series. This result further demonstrates that the electrochemical coupling between the DA oxidation and the reduction reactions plays an important role in the operation of KCl-filled CFEs. It is therefore important to understand and control the electrochemical limitations that exist at both poles of a BPE.

Limiting Current and the $E_{1/2}$ of a Closed Bipolar Microelectrode. In order to describe the limitations of the voltammetric response of a BPE, it is useful to first consider the diffusion-limited response of each pole separately. The diffusion-limited steady-state current, i_{ss} , of a planar microelectrode is described by the following equation:²⁷

$$i_{ss} = 4nFD C^* r \quad (2)$$

where n is the number of electrons transferred per molecule, F is Faraday's constant (96 485 C/mol), D is the diffusion coefficient, C^* is the bulk concentration of redox species, and r is the electrode radius. The overall voltammetric behavior of a bipolar microelectrode is expected to be dominated by the pole with a smaller predicted limiting current. This response would in fact be restricted by this "limiting pole". The other pole, capable of producing a greater current response, will be called the "excess pole".

We have constructed a closed bipolar microelectrode by connecting two 25 μm diameter Au disks in series in order to understand how its CV response depends on redox concentration. One pole is placed in a solution containing 5 mM ferricyanide and 3 M KCl while the other was in acetonitrile containing Fc of varying concentrations and 0.1 M TBAPF₆. Figure 4a shows several CVs corresponding to Fc oxidation on this bipolar microelectrode. Figure 4b shows the limiting current plotted as a function of Fc concentration. It can be seen that at concentrations ≤ 1 mM the limiting current increases linearly with Fc concentration as is predicted by eq 2. In this region the anodic pole in the Fc solution limits the overall voltammetric response. Ferrocene has a larger diffusion coefficient ($D \approx 2.4 \times 10^{-5}$ cm²/s)²⁸ than ferricyanide and thus will require a lower concentration to achieve the same limiting current. When Fc concentration is greater than 1 mM the limiting current reaches a maximum at about 19.0 nA. This "upper limit" must therefore be restricted by the reaction

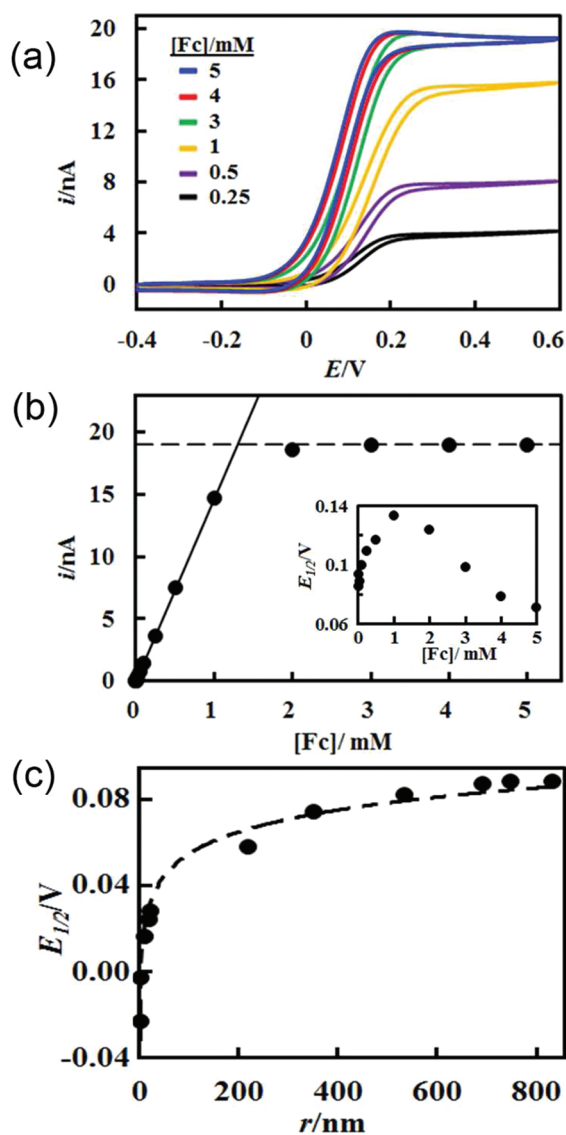


Figure 4. (a) CVs of Fc oxidation on a 25 μm diameter Au closed bipolar microelectrode as a function of Fc concentration. The other pole was a 25 μm diameter Au disk in a solution containing 5 mM $\text{Fe}(\text{CN})_6^{3-}$ and 3 M KCl. (b) The limiting current of Fc oxidation plotted vs concentration of Fc from data shown in panel a. The solid line in panel b is the linear portion where limiting current can be used to determine electrode/solution information on the Fc side. The dashed line shows limiting current on the ferricyanide side above which information is no longer obtained about the Fc side. The inset in panel b is the half-wave potential for the forward scan as a function of concentration of Fc. (c) $E_{1/2}$ as a function of Pt nanoelectrode radius for a closed bipolar setup in which a Pt nanoelectrode in MeCN containing 5 mM ferrocene, 0.1 M TBAPF₆ is connected to a 25 μm diameter Au disk electrode in 5 mM $\text{Fe}(\text{CN})_6^{3-}$ and 3 M KCl.

occurring at the cathodic pole. The limiting current for a 25 μm diameter disk electrode in 5 mM ferricyanide calculated from eq 2 is 18.4 nA. Experimentally this value was found to be slightly larger at 19.0 nA (Supporting Information Figure S11). Assuming we were using this BPE setup to study the oxidation of Fc or dopamine, we would be limited to measurements below 19.0 nA due to the limitations on the cathodic pole.

More interestingly, the change in Fc concentration has caused a noticeable shift in the position of the CV. The data presented in the inset of Figure 4b shows how the $E_{1/2}$ is

dependent on the concentration of Fc. Such behavior has been previously discussed in great detail computationally by Stewart et al.¹¹ and by Plana et al.¹⁰ We chose to revisit the topic briefly here with micro- and nanoelectrodes and later extend the concept to $E_{1/2}$ shifts due to asymmetric BPE geometries, where one pole is larger than the other. As can be seen here with an increase in Fc concentration there is initially an increase in $E_{1/2}$ from 85 mV at 10 μM Fc to 133 mV at 1 mM followed by a decrease again to 71 mV for 5 mM Fc. The trend appears to be that as the ratio of the maximum capable limiting current for the two poles (i_{ss1}/i_{ss2}), as determined separately, approaches unity the half-wave potential for the BPE approaches its maximum value, which can be approximated by eq 1.²⁹

This behavior was further examined on the basis of asymmetric BPE geometries by changing the size of the limiting pole to demonstrate that the $E_{1/2}$ shift is not merely a function of concentration ratios alone. To this end one of the 25 μm diameter Au electrodes was replaced by Pt nanoelectrodes with radii from 1 to 830 nm. The Pt nanoelectrodes were placed in 5 mM Fc, and the 25 μm Au electrode was kept in 5 mM $\text{Fe}(\text{CN})_6^{3-}$ and 3 M KCl. Figure 4c shows the $E_{1/2}$ as a function of the radius of the Pt. For the smallest Pt disk an $E_{1/2}$ of -23 mV was found, whereas the 830 nm electrode had an $E_{1/2}$ of $+88$ mV. The shift in the $E_{1/2}$ can be qualitatively explained by the following trend: an increase in the magnitude of the current demand at the limiting pole, with constant conditions at the excess pole, requires an increased voltage driving force. This translates to a requirement for a more positive potential to be applied to the anodic pole with respect to the cathodic pole. The extent to which this behavior was observed depended primarily on the initial response of the electrode used as the excess pole.

Secondary Reactions in the Voltammetric Response of Closed BPEs. Normally, only the pole with a smaller limiting current, or the limiting pole, can be studied from the overall voltammetric response. It is, however, possible to acquire information about both poles of a closed BPE from a single CV through the use of multiple redox species or "secondary" redox reactions. The series of CVs presented in Figure 5a illustrates this concept. The black and blue CVs correspond to a 25 μm diameter and a 12.5 μm diameter Au disk electrodes, respectively, both of which were obtained in an aqueous solution containing 2 mM $\text{Fe}(\text{CN})_6^{3-}/2$ mM $\text{Fe}(\text{CN})_6^{4-}$ and 1 M KCl in a conventional one-compartment cell. The limiting current for the 12.5 μm diameter electrode is approximately half that of the 25 μm electrode as expected. These two cells were then connected in series to produce a closed bipolar microelectrode. The CV obtained from this setup is also shown in Figure 5a (red). Over the region of the scan from ~ 0.1 to 0.6 V the response reaches steady state at a current, i_1 , equal to that of the 12.5 μm pole where the oxidation of ferrocyanide occurs. The reduction of ferricyanide on the 25 μm pole occurs at a rate less than its maximum capability at this point, making this the excess pole over this region of the CV. As the potential is swept beyond 0.7 V the response reaches a new higher-magnitude steady-state, i_2 , equal to the steady-state response seen at the 25 μm diameter disk alone. In this region it is clear that the 25 μm diameter cathodic pole is now limiting, but this must then require a secondary process on the 12.5 μm anodic pole to reach this elevated current. The second oxidation wave at approximately 0.7 V with respect to its ferricyanide couple would correspond to about

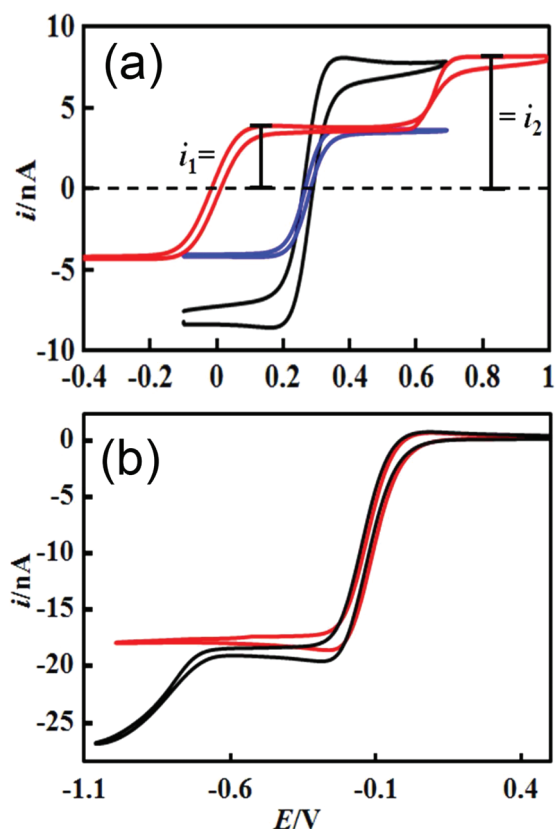


Figure 5. (a) CVs of Au microelectrodes in 2 mM $\text{Fe}(\text{CN})_6^{3-}/2$ mM $\text{Fe}(\text{CN})_6^{4-}$. The black CV is a 25 μm diameter, whereas the blue CV is a 12.5 μm diameter electrode, both in a conventional one-compartment cell. The red trace was obtained by connecting the cells containing these two electrodes in series to form a closed bipolar cell as in Figure 2a. At a potential between 0 and 0.6 V, i_1 is limited on the 12.5 μm pole by the oxidation of ferrocyanide. Above 0.7 V i_2 is limited on the 25 μm pole by the reduction of ferricyanide with the oxidation of H_2O compensating for the limitation on the 12.5 μm pole. (b) CVs of a closed bipolar cell containing two 25 μm Au electrodes in series, one in 5 mM $\text{Fe}(\text{CN})_6^{3-}$ and 3 M KCl and the other in MeCN containing 2 mM Fc and 0.1 M TBAPF₆. The wave at -0.1 V is due to the reduction of $\text{Fe}(\text{CN})_6^{3-}$. The CV in red was recorded after the solution was bubbled with N_2 . The black curve (recorded after O_2 saturation) shows ORR makes up for the limitation on the ferricyanide side to give a response limited by Fc oxidation below -1 V.

1.2 V versus NHE. It is likely that water oxidation ($2\text{H}_2\text{O} \rightarrow \text{O}_2 + 4\text{H}^+ + 4\text{e}^-$) with a standard redox potential of 1.229 V versus NHE is responsible for the process.²⁶ Supporting Information Figure SI3 shows the CV response of a 25 μm diameter Au disk electrode in the same ferricyanide/ferrocyanide mixture in a conventional setup. As the potential is swept above ~ 0.8 V the oxidation of water is observed by a large increase in current. In the bipolar experiment presented in Figure 5a this secondary reaction is limited only by the rate of the reduction of ferricyanide at the cathodic pole.

To investigate this behavior further we measured the CV response of a BPE composed of two 25 μm diameter Au disks. One electrode was immersed in a solution of 5 mM ferricyanide and 3 M KCl and the other in 2 mM Fc and 0.1 M TBAPF₆ in MeCN. The CVs presented in Figure 5b were recorded after the ferricyanide solution was oxygen-saturated (black) and after it had been deaerated with nitrogen (red). Both CVs reached their limiting current of approximately 19 nA due to the

reduction of 5 mM ferricyanide. The excess anodic pole in the Fc solution is capable of a limiting current ~ 1.3 times greater than that of the cathode pole due to the ratio of diffusion coefficients and concentrations of the two species. The reduction of O_2 must therefore be responsible for the additional wave in the black curve, making the total current approximately 26 nA, now limited by the oxidation of Fc. Supporting Information Figure SI4 shows an additional example in which a solution containing a mixture of ferricyanide and hexaamineruthenium(III) was used in series with a solution containing Fc. In the voltammogram two distinct waves with half-wave potentials of approximately -0.1 and -0.65 V were observed, for the reductions of ferricyanide and hexaamineruthenium(III), respectively. A third, less noticeable, wave can be seen at approximately -0.95 V corresponding to the ORR with an overall limiting current of 31 nA equal to what was observed for the diffusion-limited steady-state response of the Au electrode in 2 mM Fc for the conventional electrochemical cell configuration. The results shown in Figure 5 and Supporting Information Figure SI4 have demonstrated that by using a second redox reaction both poles can be studied from a single CV scan.

Platinum Bipolar Nanoelectrodes. Figure 6 shows a schematic of the experimental setup (Figure 6a) and an optical

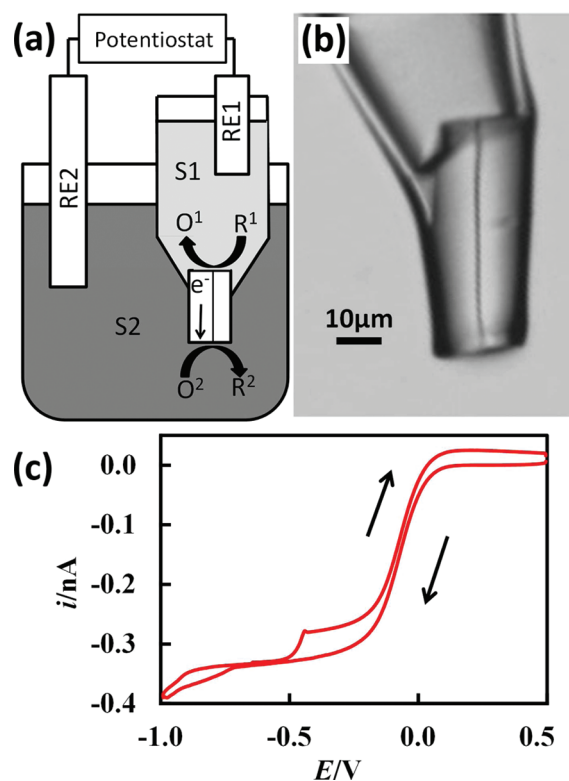


Figure 6. Schematic showing cell design (a) and optical micrograph (b) of a pipet-based Pt bipolar nanoelectrode. (c) Voltammetric response of a Pt bipolar nanoelectrode with 2 mM Fc, 0.1 M TBAPF₆ in MeCN on the inside of the pipet and 5 mM $\text{Fe}(\text{CN})_6^{3-}$ in 3 M KCl on the outside.

micrograph (Figure 6b) of one of the Pt bipolar nanoelectrodes. The voltammetric response of a BPE of this design filled with 2 mM Fc and 0.1 M TBAPF₆ and immersed in a solution of 5 mM ferricyanide and 3 M KCl is presented in Figure 6c. On the first half of the potential scan in the negative

direction the voltammetric response is relatively featureless and reaches a steady-state current of approximately -350 pA until approximately -0.75 V where the current increases slightly. On the return scan two separate well-defined waves can be seen with an overall shape similar to what was observed for the two 25 μm diameter Au electrodes shown in Figure 5b. It appears that the wave between -0.4 and -0.2 V is due to reduction of ferricyanide on the outer cathodic pole indicating a radius of approximately 210 nm of the external pole calculated from eq 2. At a potential from -0.4 to -0.9 V it is believed that the ORR occurs at the cathodic pole in addition to the reduction of ferricyanide. Previous studies on the reduction of oxygen with Pt electrodes have shown that the condition of the electrode surface and the starting potential of the scan greatly affect the ORR response.^{30,31} With the potential held at a positive voltage an oxide layer forms on the Pt, which may hinder the reduction of oxygen. In the return scan in the positive direction the ORR can now occur at more positive potentials. The ORR, being an inner-sphere electrode reaction,³² is more dependent on the condition of the electrode surface than the reduction of ferricyanide, an outer-sphere electrode reaction. Therefore, the wave due to ORR is more variable for the two scan directions.

The CV response of another pipet-based Pt BPE is shown in Supporting Information Figure SI5a for the same solutions except in this case the aqueous side was either oxygen-saturated or deaerated with nitrogen as noted. The CV for the oxygen-saturated solution shows a sigmoidal response with a limiting current of approximately -1.2 nA. Upon deaeration the CV displays the double wave similar to that seen in Figure 6 with limiting currents of -0.9 and -1.15 nA for the lower and higher waves, respectively. It appears that oxygen remaining in solution is responsible for the second reduction wave. Supporting Information Figure SI5b shows the CV of a conventional Pt nanoelectrode in 5 mM ferricyanide containing 3 M KCl. As expected the wave due to oxygen reduction can be seen in this CV as well, with the ORR occurring at a more negative potential on the initial sweep in the negative direction. Supporting Information Figure SI6 shows two additional examples of pipet-based Pt BPEs and their CVs along with corresponding SEM images. In both cases the electrode radii calculated from the CVs' distinct steady-state regions using eq 2 agree well to the dimensions measured from the corresponding SEM micrographs for the exterior poles.

CONCLUSIONS

We have shown that carbon-fiber microelectrodes are closed BPEs when backfilled with an electrolyte to establish conductivity. The direct coupling between the oxidation of redox species, e.g., dopamine, on the carbon disk and the reduction of soluble oxygen on the inner fiber is likely to be responsible for the conductivity. The voltammetric responses of micro- and nanoscale BPEs differ considerably from the response of comparable conventional electrodes. Factors that affect not only the magnitude but also the position and shape of this response include the presence of varying degrees of an excess of redox molecule at one pole as compared to the other and asymmetric pole size. We have demonstrated the ability to obtain, from a single voltammogram, quantitative measurements of the properties of both the poles of a bipolar microelectrode. This process required the use of secondary reactions such as the ORR or the presence of additional redox species. Finally, we have described the preparation and use of Pt bipolar nanoelectrodes.

ASSOCIATED CONTENT

Supporting Information

Fabrication of Pt bipolar nanoelectrodes, a table summarizing half-wave potentials and diffusion coefficients of redox species used herein, voltammetric response of additional conventional and bipolar electrodes, and SEM images of pipet-based Pt nano-BPEs. This material is available free of charge via the Internet at <http://pubs.acs.org>.

AUTHOR INFORMATION

Corresponding Author

*Phone: 206-543-1767. E-mail: zhang@chem.washington.edu.

Present Address

[†]Department of Chemistry, University of Wisconsin, 1101 University Avenue, Madison, WI 53706-1322.

ACKNOWLEDGMENTS

The authors gratefully acknowledge the University of Washington for financial support. The project or effort depicted was or is sponsored by the Department of Defense, Defense Threat Reduction Agency. The content of the information does not necessarily reflect the position or the policy of the federal government, and no official endorsement should be inferred. S.M.O. thanks the Amgen Foundation for support of an undergraduate research assistantship. We thank Stephen J. Percival for performing SEM imaging and Ernest Tomlinson for his assistance and discussions. Part of this work was conducted at the University of Washington NanoTech User Facility, a member of the National Science Foundation, National Nanotechnology Infrastructure Network (NNIN).

REFERENCES

- (1) Mavre, F.; Anand, R. K.; Laws, D. R.; Chow, K. F.; Chang, B. Y.; Crooks, J. A.; Crooks, R. M. *Anal. Chem.* **2010**, *82*, 8766–8774.
- (2) Loget, G.; Kuhn, A. *Anal. Bioanal. Chem.* **2011**, *400*, 1691–1704.
- (3) Chow, K. F.; Chang, B. Y.; Zaccaro, B. A.; Mavre, F.; Crooks, R. M. *J. Am. Chem. Soc.* **2010**, *132*, 9228–9229.
- (4) Arora, A.; Eijkel, J. C. T.; Morf, W. E.; Manz, A. *Anal. Chem.* **2001**, *73*, 3282–3288.
- (5) Mavre, F.; Chow, K. F.; Sheridan, E.; Chang, B. Y.; Crooks, J. A.; Crooks, R. M. *Anal. Chem.* **2009**, *81*, 6218–6225.
- (6) Chang, B. Y.; Mavre, F.; Chow, K. F.; Crooks, J. A.; Crooks, R. M. *Anal. Chem.* **2010**, *82*, 5317–5322.
- (7) Chow, K. F.; Mavre, F.; Crooks, R. M. *J. Am. Chem. Soc.* **2008**, *130*, 7544–7545.
- (8) Perdue, R. K.; Laws, D. R.; Hlushkou, D.; Tallarek, U.; Crooks, R. M. *Anal. Chem.* **2009**, *81*, 10149–10155.
- (9) Ndungu, P. G. Ph.D. Thesis, Drexel University, Philadelphia, PA, 2004.
- (10) Plana, D.; Jones, F. G. E.; Dryfe, R. A. W. *J. Electroanal. Chem.* **2010**, *646*, 107–113.
- (11) Stewart, A. A.; Campbell, J. A.; Girault, H. H.; Eddowes, M. *Ber. Bunsen-Ges. Phys. Chem.* **1990**, *94*, 83–87.
- (12) Hotta, H.; Akagi, N.; Sugihara, T.; Ichikawa, S.; Osakai, T. *Electrochem. Commun.* **2002**, *4*, 472–477.
- (13) Plana, D.; Shul, G.; Stephenson, M. J.; Dryfe, R. A. W. *Electrochem. Commun.* **2009**, *11*, 61–64.
- (14) Zhang, B.; Adams, K. L.; Lubser, S.; Heien, M.; Ewing, A. G. *Anal. Chem.* **2008**, *80*, 1394–1400.
- (15) Keithley, R. B.; Carelli, R. M.; Wightman, R. M. *Anal. Chem.* **2010**, *82*, 5541–5551.
- (16) Amatore, C.; Arbault, S.; Bouret, Y.; Guille, M.; Lemaitre, F.; Verchier, Y. *Anal. Chem.* **2009**, *81*, 3087–3093.

- (17) Sombers, L. A.; Hanchar, H. J.; Colliver, T. L.; Wittenberg, N.; Cans, A.; Arbault, S.; Amatore, C.; Ewing, A. G. *J. Neurosci.* **2004**, *24*, 303–309.
- (18) Bruns, D. *Methods* **2004**, *33*, 312–321.
- (19) Heien, M.; Johnson, M.; Wightman, R. *Anal. Chem.* **2004**, *76*, 5697–5704.
- (20) Ge, S.; White, G. J.; Haynes, C. L. *Anal. Chem.* **2009**, *81*, 2935–2943.
- (21) Takmakov, P.; Zachek, M. K.; Keithley, R. B.; Walsh, P. L.; Donley, C.; McCarty, G. S.; Wightman, R. M. *Anal. Chem.* **2010**, *82*, 2020–2028.
- (22) Adams, K. L.; Jena, B. K.; Percival, S. J.; Zhang, B. *Anal. Chem.* **2011**, *83*, 920–927.
- (23) Li, Y.; Bergman, D.; Zhang, B. *Anal. Chem.* **2009**, *81*, 5496–5502.
- (24) Anicet, N.; Bourdillon, C.; Moiroux, J.; Saveant, J.-M. *J. Phys. Chem. B* **1998**, *102*, 9844–9849.
- (25) von Stackelberg, M.; Pilgram, M.; Toome, W. *Z. Elektrochem.* **1953**, *57*, 342–350.
- (26) Bard, A. J.; Faulkner, L. R. *Electrochemical Methods*, 2nd ed.; John Wiley & Sons: New York, 2001.
- (27) Saito, Y. *Rev. Polarogr.* **1968**, *15*, 177–182.
- (28) Bond, A. M.; Henderson, T. L. E.; Mann, D. R.; Mann, T. F.; Thormann, W.; Zoski, C. G. *Anal. Chem.* **1988**, *60*, 1878–1882.
- (29) The ratio i_{ss1}/i_{ss2} is not intended to imply that the current passing through the two poles is different, which is in fact not the case due to the necessity of coupled electron transfer. The ratio is instead used to compare the degree to which diffusion to one pole is limiting as compared to the other.
- (30) Damjanovic, A.; Hudson, P. G. *J. Electrochem. Soc.* **1988**, *135*, 2269–2273.
- (31) Zoski, C. G.; Fernandez, J. L.; Imaduwaige, K.; Gunasekara, D.; Vadari, R. *J. Electroanal. Chem.* **2011**, *651*, 80–93.
- (32) Bard, A. J. *J. Am. Chem. Soc.* **2010**, *132*, 7559–7567.

■ NOTE ADDED AFTER ASAP PUBLICATION

This paper was published on the Web on January 25, 2012. Changes to the Acknowledgment were made, and the corrected version was reposted on January 27, 2012.